Hindawi
Wireless Communications and Mobile Computing
Volume 2018, Article ID 3497694, 8 pages
https://doi.org/10.1155/2018/3497694

Research Article

Suppressing the OFDM CFO-Caused Constellation Symbol Phase Deviation by PAPR Reduction

Adriana Lipovac,[1] **Vlatko Lipovac**,[1] **and Pamela Njemčević**[2]

[1]*Department of Electrical Engineering and Computing, University of Dubrovnik, Dubrovnik, Croatia*
[2]*Faculty of Electrical Engineering, University of Sarajevo, Sarajevo, Bosnia and Herzegovina*

Correspondence should be addressed to Adriana Lipovac; adriana.lipovac@unidu.hr

Received 5 May 2018; Revised 1 July 2018; Accepted 11 July 2018; Published 1 August 2018

Academic Editor: Sujan Rajbhandari

The well-known major drawbacks of the Orthogonal Frequency-Division Multiplexing (OFDM), namely, the transmitter versus receiver Carrier Frequency Offset (CFO), and the Peak-to-Average Power Ratio (PAPR) of the transmitted OFDM signal, may degrade the error performance, by causing Intercarrier Interference (ICI), as well as in-band distortion and adjacent channel interference, respectively. Moreover, in spite of the utmost care given to CFO estimation and compensation in OFDM wireless systems, such as wireless local networks or the mobile radio systems of the fourth generation, e.g., the Long-Term Evolution (LTE), still some residual CFO remains. With this regard, though so far the CFO and the PAPR have been treated independently, in this paper, we develop an Error Vector Magnitude (EVM) based analytical model for the CFO-induced constellation symbol phase distortion, which essentially reveals that the maximal CFO-caused squared phase deviation is linear with the instantaneous (per-OFDM-symbol) PAPR. This implies that any PAPR reduction technique, such as simple clipping or coding, indirectly suppresses the CFO-induced phase deviation, too. The analytically achieved results and conclusions are tested and successfully verified by conducted Monte Carlo simulations.

1. Introduction

Orthogonal Frequency-Division Multiplexing (OFDM) has become widely accepted due to its excellent transmission performance and high data rate under multipath fading conditions [1]. However, though OFDM performance has been subject to extensive investigations in the last two decades, specifically with regard to practical local area wireless networks (WiFi) and the fourth-generation (4G) mobile communication systems, the Long-Term Evolution (LTE) in particular [2–4], still it remains affected mainly by two OFDM drawbacks. These are the shift between the carrier frequency at the transmitter and the one used at the receiver, which is commonly referred to as Carrier Frequency Offset (CFO), and the excessive Peak-to-Average Power Ratio (PAPR) that is inherent to the transmitted OFDM signal, being effectively a sum of many sinusoids, which can mutually combine either constructively, or destructively [5, 6].

Specifically, the CFO compromises the orthogonality between subcarriers, causing mutual interference of subchannels, i.e., the Intercarrier Interference (ICI), and so severely degrades the performance. Therefore, utmost care is given to CFO estimation and compensation in OFDM wireless systems [6–9]. However, following the CFO compensation, still some residual CFO remains, which can degrade the OFDM transmission performance [1].

On the other hand, high OFDM PAPR implies large peaks of the signal that is therefore not appropriate to pass through the nonlinear High-Power Amplifier (HPA) at the transmitter, operating close to the saturation region and so introducing in-band distortion and adjacent channel interference [5].

Several methods for PAPR reduction in OFDM systems have been explored and can generally be classified as follows: clipping, coding, and distortionless, where the latter can be with or without side information sent to the receiver [10, 11].

Nevertheless, as so far the CFO and the PAPR have been treated independently, in the following, we develop an

analytical model for the constellation symbol peak CFO-induced phase deviation, which essentially reveals that reducing the OFDM PAPR indirectly suppresses the impact of the (residual) CFO, too.

In Section 2, we develop the Error Vector Magnitude (EVM) based model for the OFDM CFO-induced modulation symbol phase deviation, which, in Section 3, we find to be simply expressible in terms of PAPR. In Section 4, we verify the model by means of the Monte Carlo (MC) simulations, while conclusions are summarized in Section 5.

2. CFO-Induced EVM and Constellation Symbol Phase-Deviation Model

Consider M OFDM subchannels with complex baseband T_s-long symbols $\hat{s}_{m,n}$; $m = 1, 2, \ldots, M$, aggregated into the observed n-th transmitted OFDM symbol $\sum_{m=1}^{M} \hat{s}_{m,n} \cdot e^{jm\cdot(2\pi/MT_s)\tau}$, where τ is the sampling time. Assuming distortionless transmission, ideally, a particular k-th original symbol $\hat{s}_{k,n} = s_{k,n}e^{j\varphi_{k,n}}$ can be extracted from the incoming overall OFDM symbol $\hat{r}_{k,n}$ at the receiver, by exploiting the orthogonality within the overall OFDM symbol time MT_s, as follows [1]:

$$\begin{aligned}\hat{r}_{k,n} &= \frac{1}{MT_s}\cdot\int_{(n-1)MT_s}^{nMT_s}\left(\sum_{m=1}^{M} s_{m,n}e^{j\varphi_{m,n}}\cdot e^{jm\cdot(2\pi/MT_s)\tau}\right)\\ &\quad\cdot e^{-jk\cdot(2\pi/MT_s)\tau}d\tau\\ &= \frac{1}{MT_s}\\ &\quad\cdot\sum_{m=1}^{M} s_{m,n}e^{j\varphi_{m,n}}\cdot\int_{(n-1)MT_s}^{nMT_s} e^{j(m-k)\cdot(2\pi/MT_s)\tau}d\tau\\ &= \frac{1}{MT_s}\cdot s_{m,n}e^{j\varphi_{m,n}}\cdot\int_{0}^{MT_s} e^{j(k-k)\cdot(2\pi/MT_s)\tau}d\tau\\ &= s_{k,n}e^{j\varphi_{k,n}} = \hat{s}_{k,n}\end{aligned} \tag{1}$$

Unfortunately, a number of impairments prevent such an ideal scenario from being realistic. So, although we can justifiably consider that the cyclic prefix guard time protection against Intersymbol Interference (ISI) is sufficient to prevent long error bursts due to multipath fading [2] and also that, in many practical situations of interest, the Signal-to-Noise Ratio (SNR) is very high, implying just sporadic bit error occurrences, still the ideal detection (1) is far from reality.

With this regard, among various impairments that can degrade the physical layer transmission performance, let us consider one out of two major inherent weaknesses of OFDM systems—the CFO [1–6]. Although, strictly speaking, CFO is a random variable with certain distribution, it is always considered constant and equal for all subcarriers.

If the k-th subcarrier at the receiver exhibits the offset Δf_{CFO} with respect to the nominal transmitted frequency $k\cdot 1/MT_s$, then the detection model results in distorted actual symbol $\hat{r}_{k,n,\Delta f_{\mathrm{CFO}}}$:

$$\begin{aligned}\hat{r}_{k,n,\Delta f_{\mathrm{CFO}}} &= \frac{1}{MT_s}\\ &\quad\cdot\int_{(n-1)MT_s}^{nMT_s}\left(\sum_{m=1}^{M} s_{m,n}e^{j\varphi_{m,n}}\cdot e^{jm\cdot(2\pi/MT_s)\tau}\right)\\ &\quad\cdot e^{-j2\pi(k\cdot(1/MT_s)+\Delta f_{\mathrm{CFO}})\tau}d\tau = \frac{1}{MT_s}\\ &\quad\cdot\sum_{m=1}^{M} s_{m,n}e^{j\varphi_{m,n}}\cdot\int_{0}^{MT_s} e^{j(m-k)\cdot(2\pi/MT_s)\tau}\cdot e^{-j2\pi\Delta f_{\mathrm{CFO}}\tau}d\tau\\ &= \frac{1}{MT_s}\\ &\quad\cdot\sum_{m=1}^{M} s_{m,n}e^{j\varphi_{m,n}}\cdot\int_{0}^{MT_s} e^{j2\pi((m-k)/MT_s-\Delta f_{\mathrm{CFO}})\tau}d\tau\end{aligned} \tag{2}$$

Let us develop the integral in (2):

$$\int_0^{MT_s} e^{j2\pi((m-k)/MT_s-\Delta f_{\mathrm{CFO}})\tau}d\tau = \begin{cases}\displaystyle\int_0^{MT_s} e^{j2\pi((m-k)/MT_s-\Delta f_{\mathrm{CFO}})\tau}d\tau; & m\neq k\\ \displaystyle\int_0^{MT_s} e^{-j2\pi\Delta f_{\mathrm{CFO}}\tau}d\tau; & m=k\end{cases}$$

$$= \begin{cases}\left.\dfrac{e^{j2\pi((m-k)/MT_s-\Delta f_{\mathrm{CFO}})\tau}}{j2\pi\left((m-k)/MT_s-\Delta f_{\mathrm{CFO}}\right)}\right|_0^{MT_s} = \dfrac{e^{j2\pi(m-k-\Delta f_{\mathrm{CFO}}MT_s)}-1}{j2\pi\left((m-k)/MT_s-\Delta f_{\mathrm{CFO}}\right)} = jMT_s\dfrac{1-e^{-j2\pi\Delta f_{\mathrm{CFO}}MT_s}}{2\pi\left(m-k-\Delta f_{\mathrm{CFO}}MT_s\right)}\neq 0; & m\neq k\\ \left.\dfrac{e^{-j2\pi\Delta f_{\mathrm{CFO}}\tau}}{-j2\pi\Delta f_{\mathrm{CFO}}}\right|_0^{MT_s} = \dfrac{e^{-j2\pi\Delta f_{\mathrm{CFO}}MT_s}-1}{-j2\pi\Delta f_{\mathrm{CFO}}} = -j\dfrac{1-e^{-j2\pi\Delta f_{\mathrm{CFO}}MT_s}}{2\pi\Delta f_{\mathrm{CFO}}}\neq 1; & m=k.\end{cases} \tag{3}$$

$$1\le k\le M$$

Now, justifiably assuming that the (residual) CFO Δf_{CFO} is much smaller than the frequency increment Δf_{SC} between the neighboring subcarriers

$$\frac{\Delta f_{\mathrm{CFO}}}{\Delta f_{\mathrm{SC}}} = \Delta f_{\mathrm{CFO}} MT_s \ll 1 \Longrightarrow \Delta f_{\mathrm{CFO}} MT_s \ll 1 \tag{4}$$

then (3) becomes

$$\begin{aligned}
&\int_0^{MT_s} e^{j2\pi((m-k)/MT_s - \Delta f_{\mathrm{CFO}})\tau} d\tau \\
&\approx \begin{cases} jMT_s \dfrac{1-(1-j2\pi\Delta f_{\mathrm{CFO}} MT_s)}{2\pi(m-k)} \approx jMT_s \dfrac{-j2\pi\Delta f_{\mathrm{CFO}} MT_s}{2\pi(m-k)} = MT_s \cdot \dfrac{\Delta f_{\mathrm{CFO}} MT_s}{m-k} \approx 0; & m \neq k \\ -j\dfrac{1-1+j2\pi\Delta f_{\mathrm{CFO}} MT_s}{2\pi\Delta f_{\mathrm{CFO}}} = -j\dfrac{j2\pi\Delta f_{\mathrm{CFO}} MT_s}{2\pi\Delta f_{\mathrm{CFO}}} = MT_s; & m = k \end{cases} \qquad 1 \le k \le M
\end{aligned} \tag{5}$$

and it simplifies to

$$\begin{aligned}
&\int_0^{MT_s} e^{j2\pi((m-k)/MT_s - \Delta f_{\mathrm{CFO}})\tau} d\tau \\
&\approx \begin{cases} MT_s \cdot \dfrac{\Delta f_{\mathrm{CFO}} MT_s}{m-k} \approx 0; & m \neq k \\ MT_s; & m = k \end{cases} \qquad 1 \le k \le M
\end{aligned} \tag{6}$$

Substituting (6) into (3), the received symbol is expressed as

$$\begin{aligned}
\widehat{r}_{k,n,\Delta f_{\mathrm{CFO}}} &= \frac{1}{MT_s} \cdot \sum_{m=1}^{M} s_{m,n} e^{j\varphi_{m,n}} \\
&\cdot \int_0^{MT_s} e^{j2\pi((m-k)/MT_s - \Delta f_{\mathrm{CFO}})\tau} d\tau = \frac{1}{MT_s} \cdot \left(s_{k,n} e^{j\varphi_{k,n}} \right. \\
&\left. \cdot MT_s + \sum_{\substack{m=1 \\ m\neq k}}^{M} s_{m,n} e^{j\varphi_{m,n}} \cdot \frac{\Delta f_{\mathrm{CFO}} MT_s}{m-k} \cdot MT_s \right)
\end{aligned} \tag{7}$$

and finally as

$$\widehat{r}_{k,n,\Delta f_{\mathrm{CFO}}} = s_{k,n} e^{j\varphi_{k,n}} + \Delta f_{\mathrm{CFO}} MT_s \cdot \sum_{\substack{m=1 \\ m\neq k}}^{M} \frac{s_{m,n} e^{j\varphi_{m,n}}}{m-k} \tag{8}$$

where, in addition to the distortionless transmitted k-th symbol $\widehat{s}_{k,n}$, the second term represents the CFO-caused ISI—actually the Error Vector EV_k with magnitude EVM_k (from now on, without "n" and "Δf_{CFO}" in the indices) [2]:

$$\begin{aligned}
ISI_k = EV_k &= \Delta f_{\mathrm{CFO}} MT_s \cdot \sum_{\substack{m=1 \\ m\neq k}}^{M} \frac{s_{m,n} e^{j\varphi_{m,n}}}{m-k} \\
&= EVM_k \cdot e^{j\Phi_k} \\
EVM_k &= \Delta f_{\mathrm{CFO}} MT_s \cdot \left| \sum_{\substack{m=1 \\ m\neq k}}^{M} \frac{s_m e^{j\varphi_m}}{m-k} \right|; \quad 1 \le k \le M
\end{aligned} \tag{9}$$

Apparently, out of very large number M of subcarriers in (9) (which is justifiable assumption, e.g., with LTE), only a few neighboring symbols within the $2L \ll M$, long sliding window around the actual (k-th) symbol, really influence EV_k and so EVM_k, while the vast majority of symbols associated with the subchannels out of the window (i.e., the terms in the sum with large denominators) practically have no impact at all.

Furthermore, as M is large enough, the Central Limit Theorem applies here implying that EVM_k is a Rayleigh-distributed random variable, while the phase φ_k is uniformly distributed between $-\pi$ and π [12].

As is illustrated in Figure 1, the CFO-induced ISI_k, i.e., EV_k, actually modulates the amplitude and the phase of the received nominal (ideal) symbol, where the maximal error $\Delta\Phi_k$ of the latter occurs with EV_k perpendicular to the nominal symbol vector $\widehat{s}_k = s_k e^{j\varphi_k}$:

$$\begin{aligned}
\Delta\Phi_k &= \arctan\left(\Delta f_{\mathrm{CFO}} MT_s \cdot \frac{EVM_k}{s_k} \right) \\
&= \arctan\left(\Delta f_{\mathrm{CFO}} MT_s \right. \\
&\left. \cdot \frac{\left| \sum_{\substack{m=1 \\ m\neq k}}^{M} \left(s_m e^{j\varphi_m} / (m-k) \right) \right|}{s_k} \right); \quad 1 \le k \le M
\end{aligned} \tag{10}$$

Moreover, it is obvious in Figure 1 that $EVM_k/s_k < 1$, so, bearing in mind (4), it is also justifiable to suppose that the argument of the arctangent function in (10) is small:

$$\Delta f_{\mathrm{CFO}} MT_s \cdot \frac{EVM_k}{s_k} \ll 1 \tag{11}$$

which implies that the maximal CFO-caused phase error, expressed by (10), from now on referred to as phase deviation, becomes

$$\Delta\Phi_k \approx \Delta f_{\mathrm{CFO}} MT_s \cdot \frac{EVM_k}{s_k}$$

$$= \Delta f_{\mathrm{CFO}} M T_s \cdot \frac{\left| \sum_{\substack{m=1 \\ m \neq k}}^{M} \left(s_m e^{j\varphi_m} / (m-k) \right) \right|}{s_k}; \quad 1 \leq k \leq M \tag{12}$$

Analogously to the comment with regard to EVM_k in (9), practically only the symbols within the short, $2L \ll M$, long sliding window around the actual symbol, really influence the phase deviation $\Delta\Phi_k$.

Let us develop (12) as follows:

$$\begin{aligned}
\Delta\Phi_k &\approx \Delta f_{\mathrm{CFO}} M T_s \cdot \frac{EVM_k}{s_k} = \Delta f_{\mathrm{CFO}} M T_s \cdot \frac{\left| \sum_{\substack{m=1 \\ m \neq k}}^{M} \left(s_m e^{j\varphi_m} / (m-k) \right) \right|}{s_k} \\
&= \Delta f_{\mathrm{CFO}} M T_s \cdot \frac{\sqrt{\left(\sum_{\substack{m=1 \\ m \neq k}}^{M} \left(s_m / (m-k) \right) \cdot \cos\varphi_m \right)^2 + \left(\sum_{\substack{m=1 \\ m \neq k}}^{M} \left(s_m / (m-k) \right) \cdot \sin\varphi_m \right)^2}}{s_k} \\
&= \Delta f_{\mathrm{CFO}} M T_s \cdot \frac{\sqrt{\sum_{\substack{i=1 \\ i \neq k}}^{M} \sum_{\substack{j=1 \\ j \neq k}}^{M} \left(s_i / (i-k) \right) \cdot \left(s_j / (j-k) \right) \cos\left(\varphi_i - \varphi_j \right)}}{s_k} \\
&= \Delta f_{\mathrm{CFO}} M T_s \cdot \frac{\sqrt{\sum_{\substack{m=1 \\ m \neq k}}^{M} \left(s_m / (m-k) \right)^2 + \sum_{\substack{i=1 \\ i \neq k}}^{M} \sum_{\substack{j=1 \\ j \neq i \\ j \neq k}}^{M} \left(s_i / (i-k) \right) \cdot \left(s_j / (j-k) \right) \cos\left(\varphi_i - \varphi_j \right)}}{s_k}; \quad 1 \leq k \leq M
\end{aligned} \tag{13}$$

Actually, the terms under the square root of the numerator in (13) obviously have the form of the (weighted) mean power and the autocorrelation function, where the latter can be neglected since the symbols in the series are considered mutually statistically independent and so uncorrelated [12]:

$$\sum_{\substack{i=1 \\ i \neq k}}^{M} \sum_{\substack{j=1 \\ j \neq k \\ j \neq i}}^{M} \frac{s_i}{i-k} \cdot \frac{s_j}{j-k} \cdot \cos\left(\varphi_i - \varphi_j \right) \approx 0 \tag{14}$$

This implies that (13) reduces to

$$\Delta\Phi_k \approx \Delta f_{\mathrm{CFO}} M T_s \cdot \frac{\sqrt{\sum_{\substack{m=1 \\ m \neq k}}^{M} \left(s_m / (m-k) \right)^2}}{s_k}; \quad 1 \leq k \leq M \tag{15}$$

so that the squared CFO-caused phase deviation is

$$\Delta\Phi_k^2 \approx \left(\Delta f_{\mathrm{CFO}} M T_s \right)^2 \cdot \frac{\sum_{\substack{m=1 \\ m \neq k}}^{M} \left(s_m / (m-k) \right)^2}{s_k^2} \tag{16}$$

Moreover, it is the peak CFO-induced phase deviation $\Delta\Phi_{k\,\max}$, obtained from (16):

$$\Delta\Phi_{k\,\max}^2 \approx \left(\Delta f_{\mathrm{CFO}} M T_s \right)^2 \cdot \frac{\max_m \left\{ \sum_{\substack{m=1 \\ m \neq k}}^{M} \left(s_m^2 / (m-k)^2 \right) \right\}}{s_k^2}; \quad 1 \leq k \leq M \tag{17}$$

which is most likely to make the observed symbol $\hat{s}_k$ erroneous, where the numerator is maximal when the high-amplitude outer constellation symbols dominate the observed data sequence window. This is even more pronounced if s_k in denominator is small, i.e., if it belongs to the most inner symbols in constellation, and/or when its subchannel is more faded than the other ones. (OFDM's main task is to enable flat intrasubchannel fading, while allowing intersubchannel fading variation.)

3. Peak CFO-Induced Phase Deviation versus PAPR Model

In order to estimate $\Delta\Phi_{k\,\max}^2$, let us recall that the 4-, 16-, and 64-QAM symbols with maximal amplitudes have both I and Q component equal to 1, 3, and 7, respectively, normalized, i.e., divided by $\sqrt{2}$, $\sqrt{10}$, and $\sqrt{42}$, respectively (so that the mean symbol energy equals 1) [13]:

$$s_{m,\max 4-\mathrm{QAM}}^2 = \frac{1}{2} \cdot \left(1^2 + 1^2 \right) = 1$$

$$s_{m,\max 16-\mathrm{QAM}}^2 = \frac{1}{10} \cdot \left(3^2 + 3^2 \right) = 1.8: \quad 1 \leq m \leq M$$

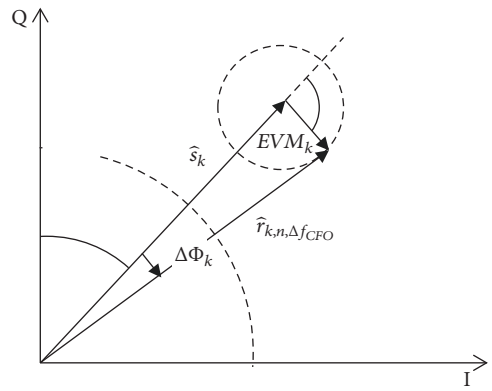

Figure 1: OFDM CFO-induced modulation symbol phase error model.

$$s^2_{m,\max 64-\mathrm{QAM}} = \frac{1}{42}\cdot\left(7^2+7^2\right)\approx 2.33 \tag{18}$$

Then, the numerator in (17) can be maximized by $s_m^2; 1 \le k \le M$ taking only the peak values from (18) weighted by the probabilities of s_m belonging to a specific modulation:

$$\begin{aligned}
&P\left(s_m = \frac{s_{m,\max 4-\mathrm{QAM}}}{s_m} \in 4-\mathrm{QAM}\right)\\
&\quad\cdot P\left(s_m \in 4-\mathrm{QAM}\right) = 1\cdot P\left(s_m \in 4-\mathrm{QAM}\right)\\
&\quad = P\left(s_m \in 4-\mathrm{QAM}\right)\\
&P\left(s_m = \frac{s_{m,\max 16-\mathrm{QAM}}}{s_m} \in 16-\mathrm{QAM}\right)\\
&\quad\cdot P\left(s_m \in 16-\mathrm{QAM}\right) = 1\cdot P\left(s_m \in 16-\mathrm{QAM}\right)\\
&\quad = P\left(s_m \in 16-\mathrm{QAM}\right)\\
&P\left(s_m = \frac{s_{m,\max 64-\mathrm{QAM}}}{s_m} \in 64-\mathrm{QAM}\right)\\
&\quad\cdot P\left(s_m \in 64-\mathrm{QAM}\right) = 1\cdot P\left(s_m \in 64-\mathrm{QAM}\right)\\
&\quad = P\left(s_m \in 64-\mathrm{QAM}\right)
\end{aligned} \tag{19}$$

So, taking into account (18) and (19), (17) develops as

$$\Delta\Phi^2_{k\max} \approx \Delta f^2_{\mathrm{CFO}} \cdot \frac{\sum_{\substack{m=1\\ m\neq k}}^{M}\left(P\left(s_m \in 4-\mathrm{QAM}\right)\cdot s^2_{m,\max 4-\mathrm{QAM}} + P\left(s_m \in 16-\mathrm{QAM}\right)\cdot s^2_{m,\max 16-\mathrm{QAM}} + P\left(s_m \in 64-\mathrm{QAM}\right)\cdot s^2_{m,\max 64-\mathrm{QAM}}\right)/(m-k)^2}{s_k^2}; \quad 1\le k\le M \tag{20}$$

Here we recall that the expression in the numerator of the sum in (20) is actually the weighted instantaneous *PAPR* for the OFDM symbol [12], as it takes into account the maximal values of all 3 LTE M-ary QAM modulation symbol amplitudes, weighted by their corresponding probabilities of appearance in the OFDM symbol:

$$\begin{aligned}
PAPR_k &= \frac{P_{peak}}{P_{avg}} = \frac{\max_m\left\{(1/2)\cdot\sum_{m=1}^{M} s_m^2\right\}}{(1/2)\cdot\sum_{m=1}^{M} s_m^2}\\
&= \frac{M\cdot\left[P\left(s_m \in 4-\mathrm{QAM}\right)\cdot s^2_{m,\max 4-\mathrm{QAM}} + P\left(s_m \in 16-QAM\right)\cdot s^2_{m,\max 16-\mathrm{QAM}} + P\left(s_m \in 64-\mathrm{QAM}\right)\cdot s^2_{m,\max 64-\mathrm{QAM}}\right]}{\sum_{m=1}^{M} s_m^2}\\
&= \frac{P\left(s_m \in 4-\mathrm{QAM}\right)\cdot s^2_{m,\max 4-\mathrm{QAM}} + P\left(s_m \in 16-\mathrm{QAM}\right)\cdot s^2_{m,\max 16-\mathrm{QAM}} + P\left(s_m \in 64-\mathrm{QAM}\right)\cdot s^2_{m,\max 64-\mathrm{QAM}}}{E\left[s_k^2\right]}
\end{aligned} \tag{21}$$

where we substituted (18) and took into account that the mean energies of 4-, 16-, and 64-QAM original symbols are all normalized to 1; i.e.,

$$E\left[s_k^2\right] = 1 \tag{22}$$

so that (21) finally becomes

$$\begin{aligned}
PAPR_k = {} & P\left(s_m \in 4-\mathrm{QAM}\right)\cdot 1\\
& + P\left(s_m \in 16-\mathrm{QAM}\right)\cdot 1.8\\
& + P\left(s_m \in 64-\mathrm{QAM}\right)\cdot 2.33; \quad 1\le k\le M
\end{aligned} \tag{23}$$

Consequently, (20) can be expressed as

$$\Delta\Phi_{k\max}^2 \approx \left(\Delta f_{\mathrm{CFO}} M T_s\right)^2 \cdot \frac{PAPR_k}{s_k^2} \cdot \sum_{\substack{m=1 \\ m\neq k}}^{M} \frac{1}{(m-k)^2}; \quad 1 \le k \le M \tag{24}$$

Now let us calculate the sum in (24), where, actually, just the neighboring $2L$ terms, rather than all M-1 ones, determine $\Delta\Phi_{k\max}^2$, as the remaining terms, divided by the increased $(m-k)^2$ denominators, soon become negligible. We consider adopting L=6 justifiable, neglecting terms lesser than 5% of the central one:

$$\begin{aligned}
\sum_{\substack{m=1 \\ m\neq k}}^{M} \left(\frac{1}{m-k}\right)^2 &= \frac{1}{(1-k)^2} + \frac{1}{(2-k)^2} + \cdots \\
&\quad + \frac{1}{[(k-5)-k]^2} + \frac{1}{[(k-4)-k]^2} \\
&\quad + \frac{1}{[(k-3)-k]^2} + \frac{1}{[(k-2)-k]^2} \\
&\quad + \frac{1}{[(k-1)-k]^2} + + \frac{1}{[(k+1)-k]^2} \\
&\quad + \frac{1}{[(k+2)-k]^2} + \frac{1}{[(k+3)-k]^2} \\
&\quad + \frac{1}{[(k+4)-k]^2} + \frac{1}{[(k+5)-k]^2} \\
&\quad + \cdots + \frac{1}{[(M-1)-k]^2} + \frac{1}{(M-k)^2} \\
&\approx \frac{1}{6^2} + \frac{1}{5^2} + \frac{1}{4^2} + \frac{1}{3^2} + \frac{1}{2^2} + \frac{1}{1^2} + \frac{1}{1^2} \\
&\quad + \frac{1}{2^2} + \frac{1}{3^2} + \frac{1}{4^2} + \frac{1}{5^2} + \frac{1}{6^2} \\
&= 2 \cdot \left(\frac{1}{36} + \frac{1}{25} + \frac{1}{16} + \frac{1}{9} + \frac{1}{4} + 1\right) \\
&= 2.98256
\end{aligned} \tag{25}$$

i.e.,

$$\sum_{\substack{m=1 \\ m\neq k}}^{M} \left(\frac{1}{m-k}\right)^2 \approx 2 \cdot \sum_{i=1}^{6} \frac{1}{i^2} \approx 3 \tag{26}$$

This implies

$$\Delta\Phi_{k\max}^2 \approx 3 \cdot PAPR_k \cdot \frac{\left(\Delta f_{\mathrm{CFO}} M T_s\right)^2}{s_k^2}; \quad 1 \le k \le M \tag{27}$$

It can be seen that the CFO-caused maximal squared phase deviation $\Delta\Phi_{k\max}^2$ is linear with the instantaneous (per-OFDM-symbol) *PAPR*, implying that any PAPR reduction technique, such as simple clipping, indirectly suppresses the CFO-induced phase deviation and so the consequent ISI.

This applies to expectedly small residual (postcompensation) CFO, even with maximal number of subchannels (2048 in LTE), but also enables considerable reduction of the noncompensated CFO-induced phase deviation, especially for smaller number of subchannels (when (4) holds even more likely), to the extent that PAPR reduction is taken care of, e.g., by simple clipping or coding.

Consequently, the CFO compensation task can be either enhanced by PAPR reduction or even completely assigned to it, thus enabling simplification of the receiver processing.

Moreover, as for a small-amplitude actual symbol (in denominator of (24)), $\Delta\Phi_{k\max}^2$ gets larger, and this unveils the need to equalize the transmission quality for all constellation points by some kind of digital preemphasis of the lower-amplitude modulation symbols, i.e., the "inner" constellation states. It might be that a metric-based symbol predistortion [14] or effective combining of PAPR reduction and HPA predistortion techniques could enable performance optimization with this regard.

Furthermore, instead of (21)/(23), adopting the per-(M-long)-OFDM-symbol *PAPR* determined by the absolutely maximal subchannel symbol (of 64-QAM)

$$\begin{aligned}
PAPR_{k\mathrm{abs}} &= \frac{M \cdot s_{m,\max 64-\mathrm{QAM}}^2}{\sum_{m=1}^{M} s_m^2} = \frac{s_{m,\max 64-\mathrm{QAM}}^2}{\sum_{m=1}^{M} s_m^2/M} \\
&= \frac{2.33}{E\left[s_k^2\right]} = 2.33; \quad 1 \le k \le M
\end{aligned} \tag{28}$$

and then substituting (28) into (27) lead to the absolute maximal CFO-induced peak phase deviation:

$$\Delta\Phi_{k\mathrm{abs}\,\max} \approx \sqrt{7} \cdot \frac{\Delta f_{\mathrm{CFO}} M T_s}{s_k}; \quad 1 \le k \le M \tag{29}$$

4. Verification of Peak CFO-Induced Phase Deviation

In order to verify the developed analytical model, we estimated the CFO-induced squared phase deviation by both (23)/(27) and (29) and compared the results with the corresponding ones obtained by MC simulations.

In the first case, it is necessary to previously adopt the probabilities that a symbol belongs to a particular modulation used in LTE systems. The prerequisite for realistic assumption with this regard is a reliable preceding traffic analysis, or taking the data from literature. As such comprehensive data analysis is out of scope of this work, we adopt the following exemplar values [15]:

$$\begin{aligned}
P\left(s_m \in 4-\mathrm{QAM}\right) &= 0.4 \\
P\left(s_m \in 16-\mathrm{QAM}\right) &= 0.5 \\
P\left(s_m \in 64-\mathrm{QAM}\right) &= 0.1
\end{aligned} \tag{30}$$

Then, by substituting (30) into (23), we obtain

$$PAPR_k = 0.4 \cdot 1 + 0.5 \cdot 1.8 + 0.1 \cdot 2.33 = 1.533 \tag{31}$$

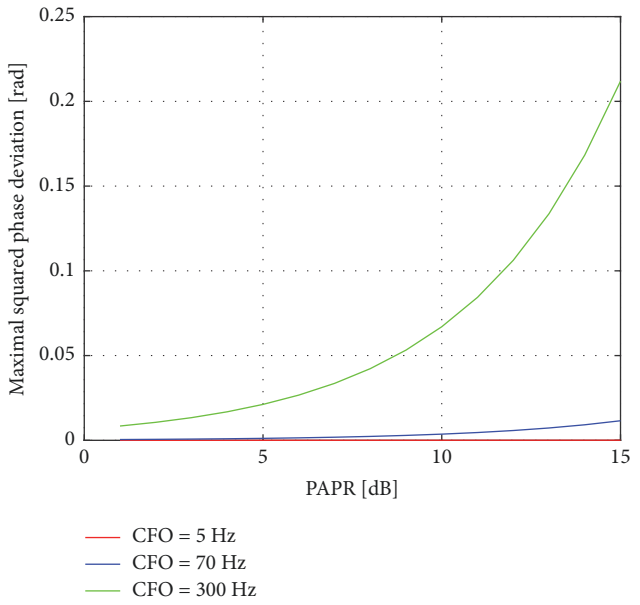

FIGURE 2: Maximal squared phase deviation versus instantaneous *PAPR* (27), dispersion with CFO; M=2048, $1/T_s$=13 Mbps.

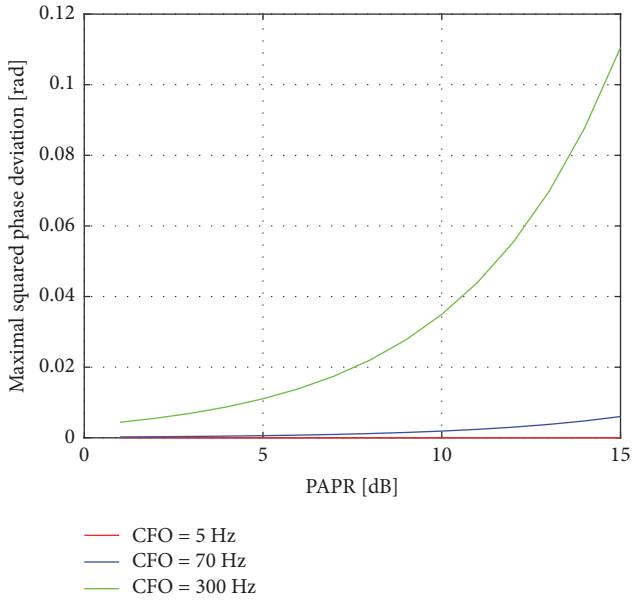

FIGURE 3: Maximal squared phase deviation versus instantaneous *PAPR* (27), dispersion with CFO; M=2048, $1/T_s$=18 Mbps.

which is inserted into (27) to finally result in

$$\Delta\Phi_{k\,\max} \approx \sqrt{4.6} \cdot \frac{\Delta f_{\mathrm{CFO}} M T_s}{s_k}; \quad 1 \le k \le M \qquad (32)$$

Accordingly, the graphs for the exemplar CFO values: 0 Hz, 5 Hz, 70 Hz, and 300 Hz [1], and unit observed symbol amplitude s_k, are presented in Figures 2-3, following (27) for the rates of 13 and 18 Mbps, respectively.

As it can be seen in each of these figures alone, the CFO-induced modulation symbol phase-deviation-versus-*PAPR* curves dispersion with rising CFO becomes considerable. Similarly, by observing interfigures, it is evident that increasing the bit-rate effectively reduces the phase deviation.

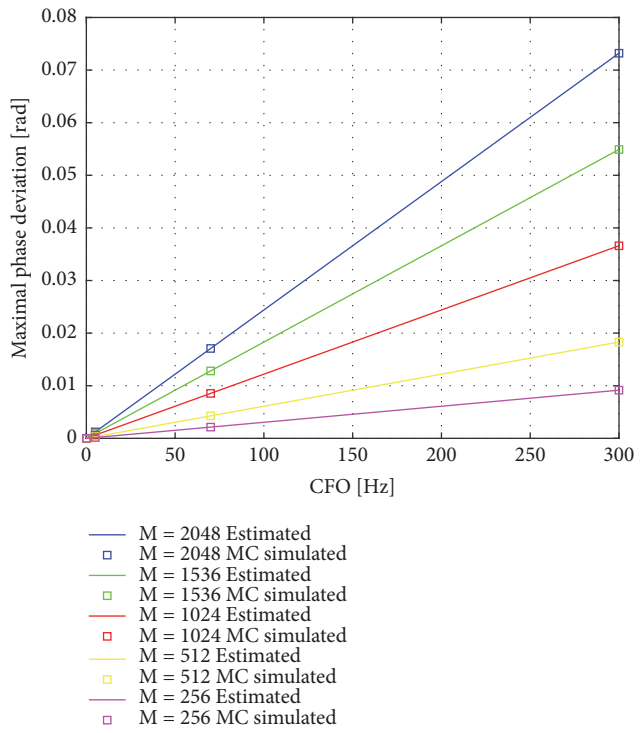

FIGURE 4: Maximal phase deviation versus CFO (32); M=2048, $1/T_s$=18 Mbps.

Furthermore, in Figures 4-5, the phase-deviation curves dispersion is evident with M increasing from the minimal to the (worst-case) maximal value used in LTE. Excellent matching between the values estimated according to (29) and (32), and the MC-simulated ones, can be seen, which verifies the model and its implications, as well.

Moreover, the analytically predicted plots as well as the corresponding MC-simulated ones, reflect the linear relationship between the CFO-caused symbol phase deviation and the *PAPR*.

5. Conclusion

Two major inherent weaknesses of the OFDM-based state-of-the art wireless systems, such as the LTE, are CFO and PAPR, which compromise the orthogonality of subcarriers and introduce cochannel and adjacent channel interference, respectively. Therefore, CFO compensation as well as PAPR reduction has been advocated for two decades, through a number of proposed methods treating CFO or PAPR mutually exclusively and independently of each other.

However, with this regard, we develop an EVM-based analytical model for the constellation symbol phase, unveiling that the CFO-caused maximal squared phase deviation is linear with the instantaneous (per-OFDM-symbol) PAPR. Moreover, this implies that any PAPR reduction technique,

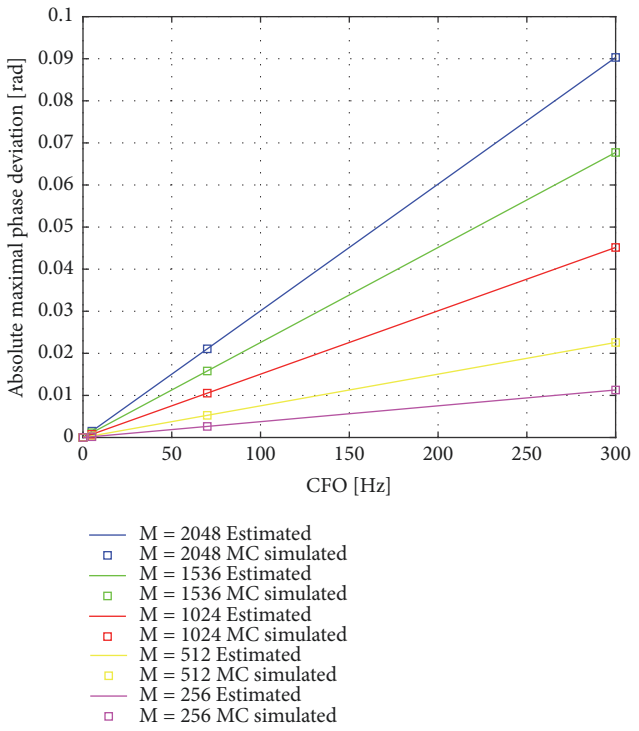

FIGURE 5: Absolute maximal phase deviation versus CFO (29); M=2048, $1/T_s$=18 Mbps.

such as simple clipping, indirectly suppresses the CFO-induced phase deviation, too.

The model is developed on the ground of justifiable assumption (e.g., with LTE) that the CFO is much smaller than the frequency increment between the neighboring OFDM subcarriers and that only a few neighboring symbols within the narrow window around the actual symbol really influence its EVM.

This applies to small residual (postcompensation) CFO, even with maximal number of subchannels (2048 in LTE), but also enables significant reduction of the noncompensated CFO-induced phase deviation (to the extent that PAPR reduction is taken care of), especially for smaller number of subchannels.

Consequently, the CFO compensation task can be either enhanced by PAPR reduction or even completely assigned to it, thus enabling simplification of the receiver processing.

The theoretical model is tested and successfully verified by Monte Carlo simulations, which implies the validity of the above stated model implications on the receiver design, as well.

Data Availability

The data used to support the findings of this study are available from the corresponding author upon request.

Conflicts of Interest

The authors declare that they have no conflicts of interest.

References

[1] A. Lipovac, V. Lipovac, and B. Modlic, "Modeling OFDM irreducible BER with impact of CP length and CFO in multipath channel with small delay dispersion," *Wireless Communications and Mobile Computing*, vol. 16, no. 9, pp. 1065–1077, 2016.

[2] M. Rumnay, *LTE and the Evolution of 4G Wireless; Design and Measurements Challenges*, John Wiley & Sons, 2nd edition, 2013.

[3] A. Molisch, *Wireless Communications*, Wiley, New York, NY, USA, 2nd edition, 2011.

[4] L. Korowajczuk, "LTE, WIMAX and WLAN Network Design, Optimization and Performance Analysis," *LTE, WIMAX and WLAN Network Design, Optimization and Performance Analysis*, 2011.

[5] R. Prasad, *OFDM for Wireless Communications Systems*, Artech House, Boston, Mass, USA, 2004.

[6] H. A. Ahmed, A. I. Sulyman, and H. S. Hassanein, "Bit error rate performance of orthogonal frequency-division multiplexing relaying systems with high power amplifiers and Doppler effects," *Wireless Communications and Mobile Computing*, vol. 13, no. 8, pp. 734–744, 2013.

[7] S. Mohseni and M. A. Matin, "Study of the Sensitivity of the OFDM Wireless Systems to the Carrier Frequency Offset (CFO)," *International Journal of Distributed and Parallel Systems*, vol. 4, no. 1, pp. 1–13, 2013.

[8] H. Steendam and M. Moeneclaey, "Sensitivity of orthogonal frequency-division multiplexed systems to carrier and clock synchronization errors," *Signal Processing*, vol. 80, no. 7, pp. 1217–1229, 2000.

[9] P. H. Moose, "Technique for orthogonal frequency division multiplexing frequency offset correction," *IEEE Transactions on Communications*, vol. 42, no. 10, pp. 2908–2914, 1994.

[10] T. Jiang and Y. Wu, "An overview: peak-to-average power ratio reduction techniques for OFDM signals," *IEEE Transactions on Broadcasting*, vol. 54, no. 2, pp. 257–268, 2008.

[11] S. H. Han and J. H. Lee, "An overview of peak-to-average power ratio reduction techniques for multicarrier transmission," *IEEE Wireless Communications Magazine*, vol. 12, no. 2, pp. 56–65, 2005.

[12] D. Drajic, *Introduction to Statistical Theory of Telecommunications*, Akademic Thought, Belgrade, Serbia, 2nd edition, 2006.

[13] J. R. Barry, E. A. Lee, and D. G. Messerschmitt, *Digital Communication*, vol. 3rd, Springer, Boston, MA, USA, 2004.

[14] S. Sezginer and H. Sari, "Metric-based symbol predistortion techniques for peak power reduction in OFDM systems," *IEEE Transactions on Wireless Communications*, vol. 6, no. 7, pp. 2622–2629, 2007.

[15] J. C. Ikuno, C. Mehlfuhrer, and M. Rupp, "A Novel Link Error Prediction Model for OFDM Systems with HARQ," in *Proceedings of the ICC 2011 - 2011 IEEE International Conference on Communications*, pp. 1–5, Kyoto, Japan, June 2011.